

Allostery governs Cdk2 activation and differential recognition of CDK inhibitors

Abir Majumdar^{1#}, David J. Burbán^{1#}, Joseph M. Muretta², Andrew R. Thompson², Tiffany A. Engel¹, Damien M. Rasmussen¹, Manu V. Subrahmanian², Gianluigi Veglia², David D. Thomas² and Nicholas M. Levinson^{1*}

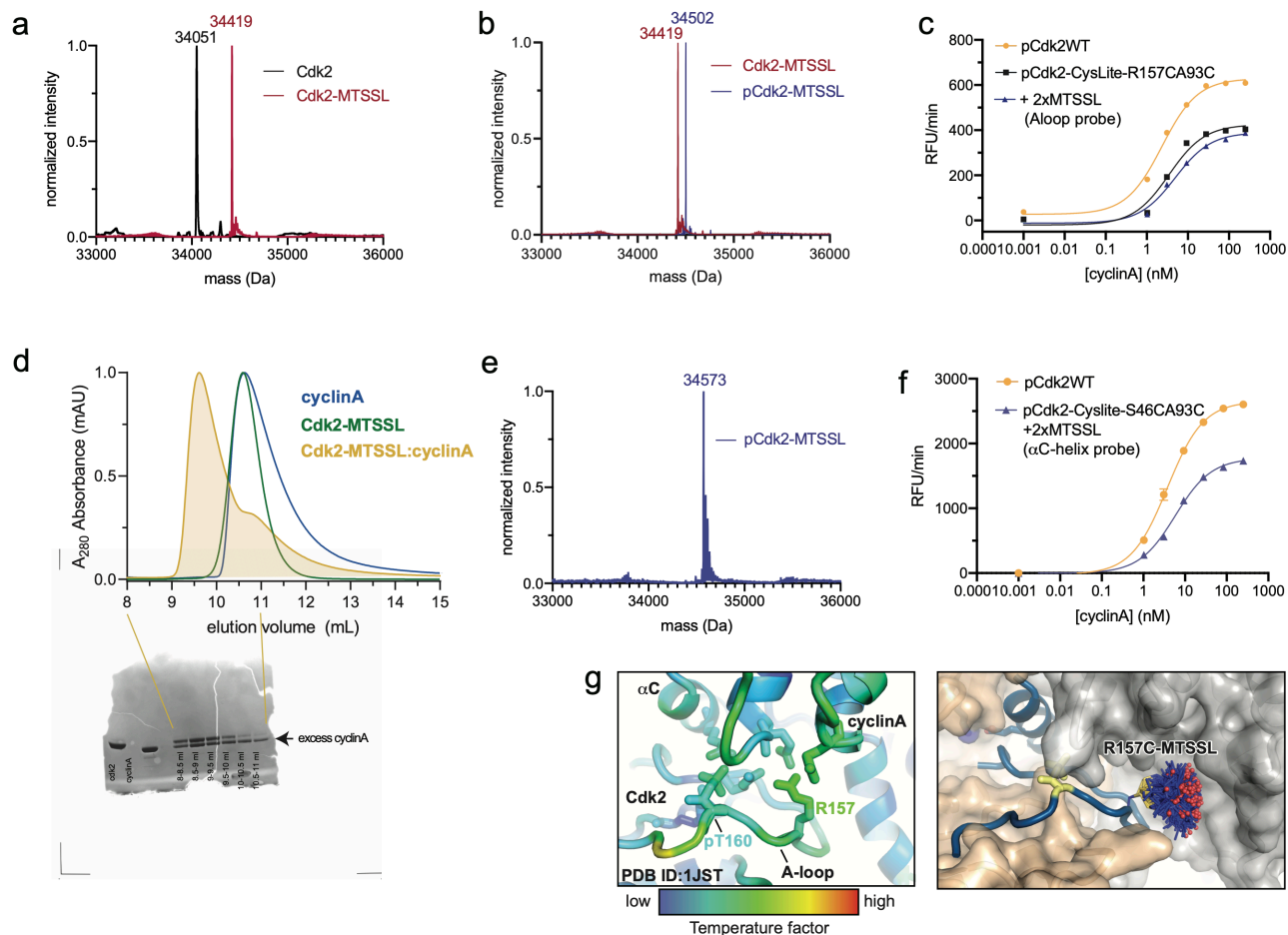
¹Department of Pharmacology and Masonic Cancer Center, University of Minnesota, 312 Church St. SE., Minneapolis, MN 55455

²Department of Biochemistry, Molecular Biology, and Biophysics, University of Minnesota, 312 Church St. SE, Minneapolis, MN 55455

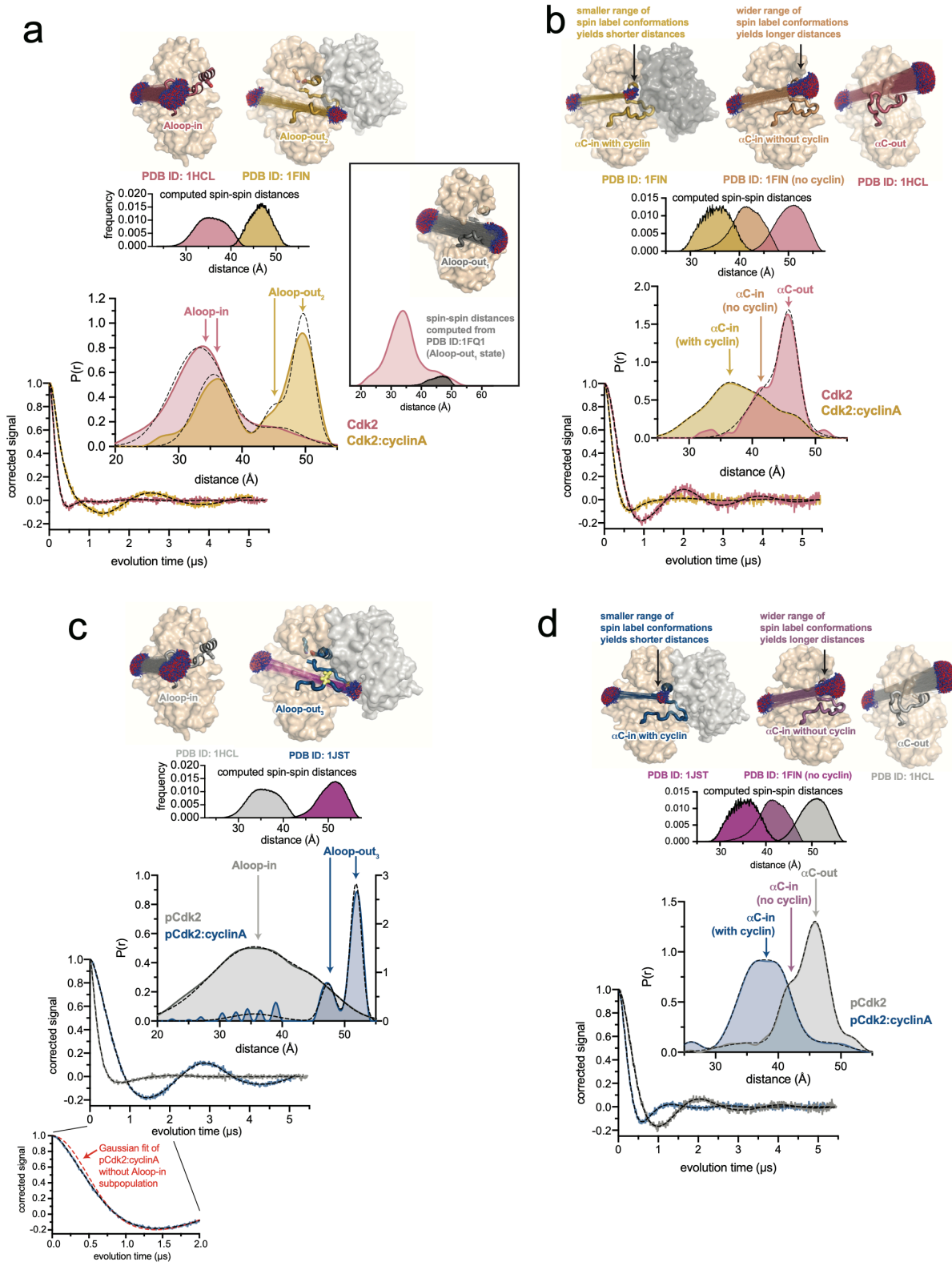
*To whom correspondence should be addressed (nml@umn.edu)

#These authors contributed equally to this work

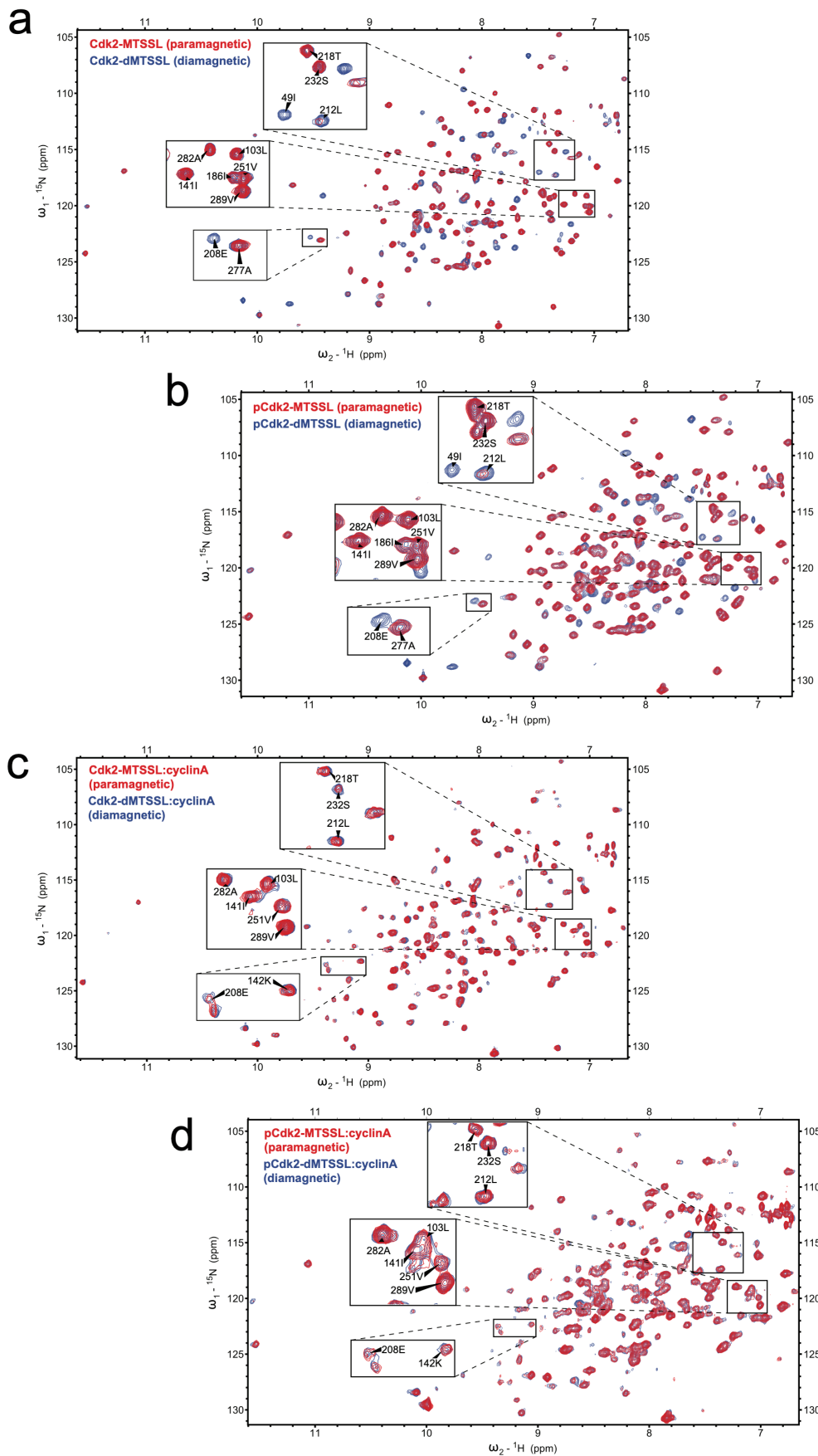
Supplementary Figures



Supplementary Figure 1. Validation of MTSSL-labeled Cdk2 phosphorylation, labeling and function. **a)** Mass spectra of unphosphorylated Cdk2 (DEER A-loop construct) without (black) and with (red) two MTSSL spin probes (+368 Da). Expected masses: 34,054 Da and 34,422 Da, respectively. **b)** Mass spectra of unphosphorylated (red) and phosphorylated (blue) Cdk2 (DEER A-loop construct) labeled with two MTSSL labels on A93C and R157C. **c)** Kinase activity assays showing catalytic activation of Cdk2 WT, the unlabeled DEER A-loop construct (Cdk2-Cyslite-R157CA93C), and the DEER A-loop construct labeled with 2 MTSSL spin labels. We confirmed that the spin labels remained on the kinase in the kinase activity assay buffer by mass spectrometry. **d)** Size exclusion chromatography traces for unphosphorylated spin-labeled monomeric Cdk2 (DEER A-loop construct) (red) and Cdk2:cyclinA dimer (yellow) as well as free cyclinA (blue), demonstrating that the spin-labeled kinase binds the cyclinA subunit. The SDS-PAGE gel shows fractions from the Cdk2:cyclinA dimer run confirming formation of the 1:1 complex and demonstrating that the sample was prepared with excess cyclinA. Protein samples used for reference Cdk2 and cyclinA markers (lanes 1 and 2) had been previously validated. This analysis was performed on the sample used for the DEER experiment. **e)** Mass spectrum of the phosphorylated Cdk2 α C-helix construct with two MTSSL labels on S46C and A93C. Expected mass: 34,573 Da. **f)** Kinase activity assays showing catalytic activity of the α C-helix probe construct compared to WT Cdk2. The activity of the +2xMTSSL sample was measured with protein previously used in the DEER experiment itself. **g)** Crystallographic temperature factors (left) and spin label conformational modeling (right) of the A-loop labeling site residue R157.

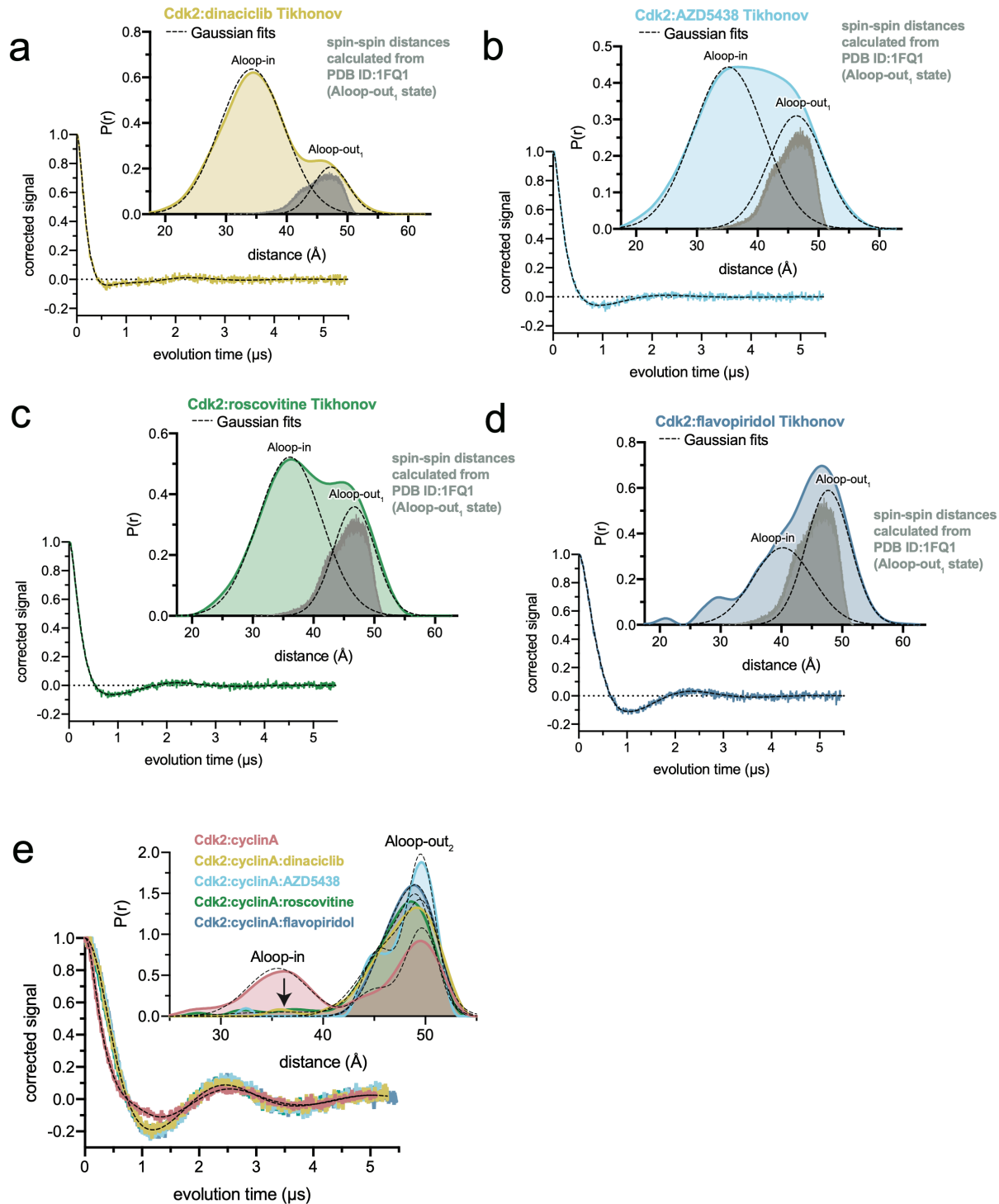


Supplementary Figure 2. Gaussian fits of the DEER spectra can be assigned to specific conformational states of Cdk2 observed in x-ray structures. MTSSL rotamers visualized on the x-ray structures of Cdk2 using the PyMOL plugin MtsslWizard. Calculated ensemble distance distributions were used to assign conformational states to Gaussian populations from the DEER experiments measuring **a**) the A-loop of Cdk2 and Cdk2:cyclinA, showing that Cdk2 samples the Aloop-out₁ state (inset), and that Cdk2:cyclinA adopts the Aloop-out₂ state, **b**) the α C-helix of Cdk2 and Cdk2:cyclinA, showing that the MTSSL probe is more constrained in the presence of cyclin, leading to different Gaussian centers for the α C-in conformation, **c**) the A-loop of pCdk2 and pCdk2:cyclinA, showing that pCdk2 has a similar Aloop-out subpopulation to Cdk2 and that pCdk2:cyclinA adopts the Aloop-out₃ state, **d**) the α C-helix of pCdk2 and pCdk2:cyclinA, showing that pCdk2:cyclinA is mostly shifted to the α C-in state. The inset in c shows the result of attempting to fit the pCdk2:cyclinA DEER data without the Aloop-in subpopulation (red), highlighting that the Aloop-in subpopulation is necessary to fit the early evolution times.

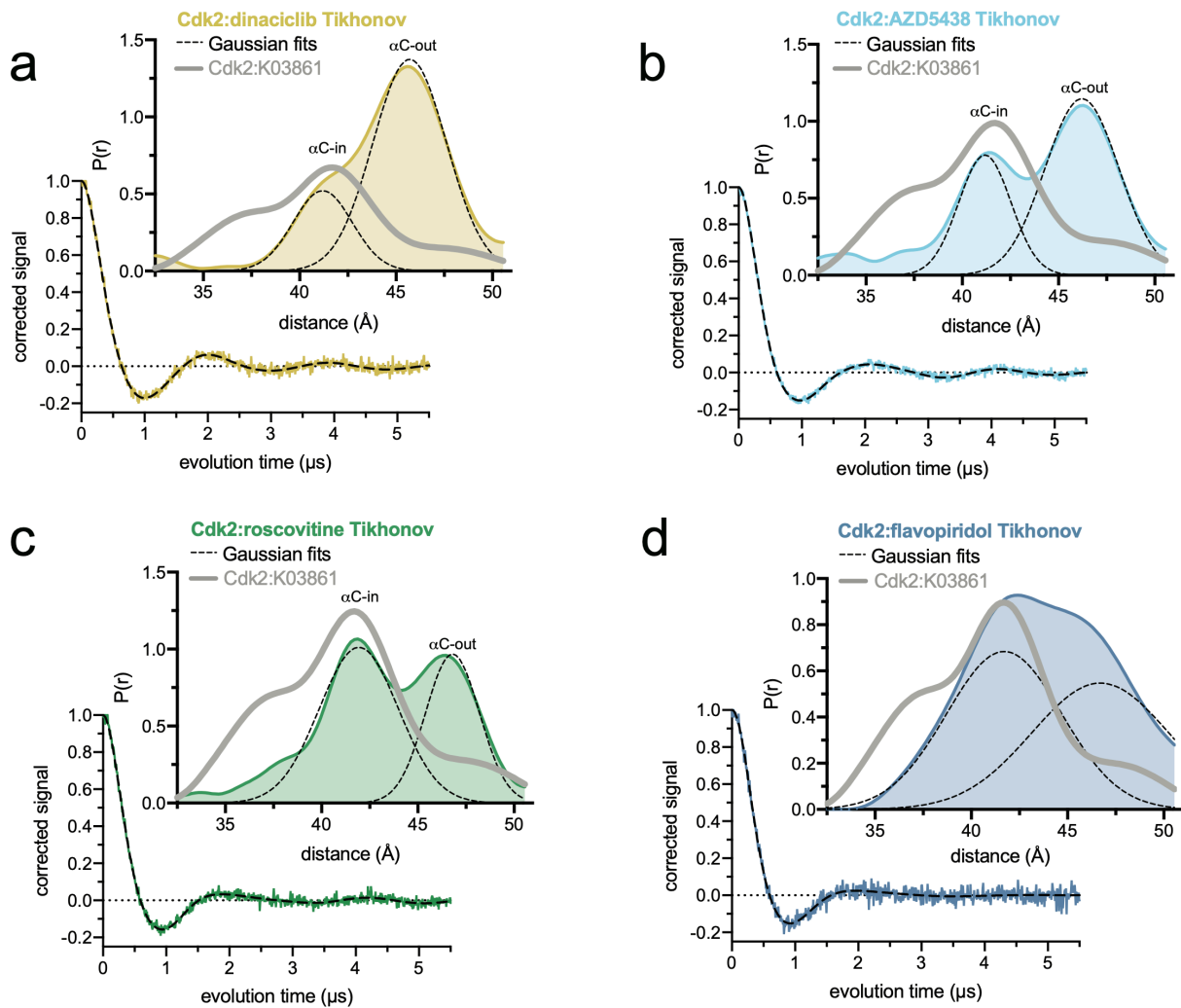


Supplementary Figure 3. NMR spectra of MTSSL- and dMTSSL-labeled Cdk2. The TROSY-HSQC spectra of MTSSL-labeled (paramagnetic) and dMTSSL-labeled (diamagnetic) Cdk2 samples in the four biochemical states are shown. Resonance assignments are shown in the insets. **a**) Monomeric unphosphorylated Cdk2 (Cdk2). **b**) Monomeric phosphorylated Cdk2 (pCdk2). **c**) Unphosphorylated Cdk2:cyclinA dimer (Cdk2:cyclinA), **d**) Phosphorylated Cdk2:cyclinA dimer (pCdk2:cyclinA).

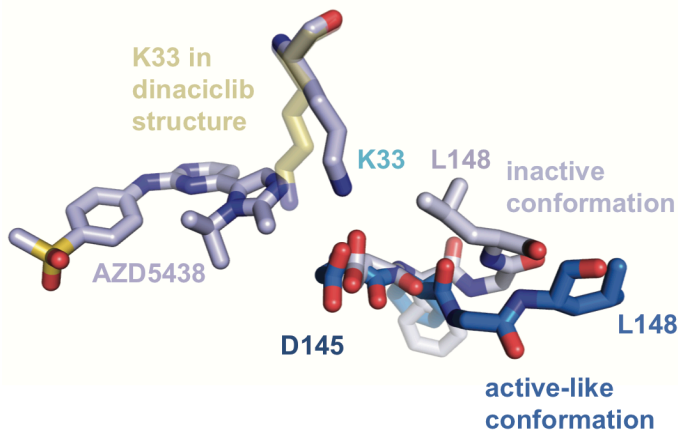
values for pCdk2:cyclinA. The experimental values are consistent with adoption of the Aloop-out₃ state, as well as the loss of the Aloop-in subpopulation seen in the absence of phosphorylation. Error bars represent the standard error calculated from the signal-to-noise ratio of the entire spectrum.



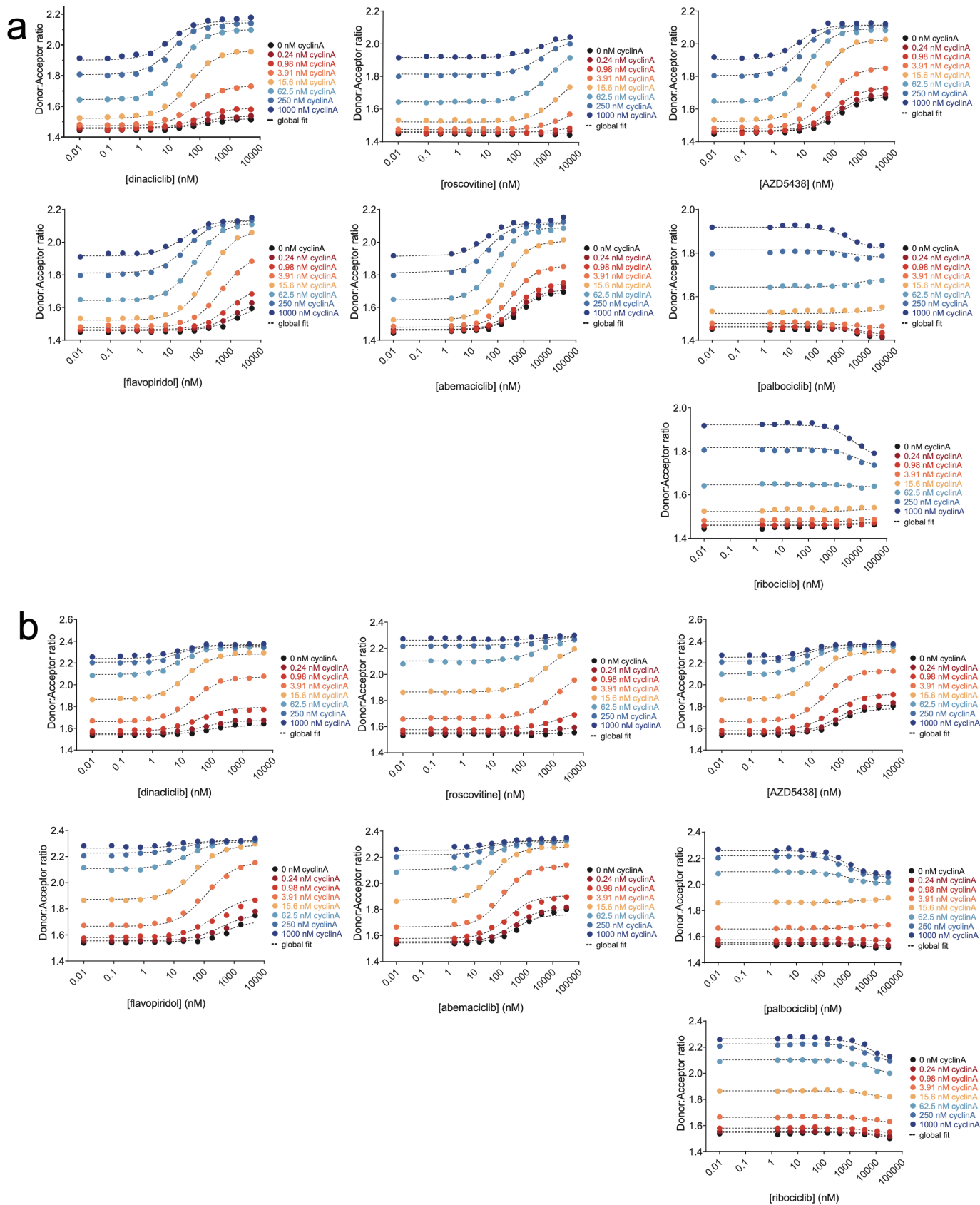
Supplementary Figure 5. DEER data on unphosphorylated Cdk2 bound to Cdk2 inhibitors (Aloop). DEER spectra (bottom) and spin-spin distance distributions (top) for Cdk2 bound to four Cdk2 inhibitors. Distance distributions were acquired by fitting DEER spectra using Tikhonov regularization, and independently fitting to two Gaussian functions representing Aloop-in and Aloop-out₁ states. The calculated Aloop-out₁ distance distribution from the Cdk2:KAP structure (1FQ1) is shown in grey and scaled along the y-axis for clarity. DEER spectra, Tikhonov fits and decomposed Gaussian fits are shown for **a**) Cdk2:dinaciclilb, **b**) Cdk2:AZD5438, **c**) Cdk2:roscovitine, **d**) Cdk2:flavopiridol. **e**) All four inhibitors promote the Aloop-out₂ state in the presence of cyclinA, as manifested by a loss of the Aloop-in subpopulation (arrow).



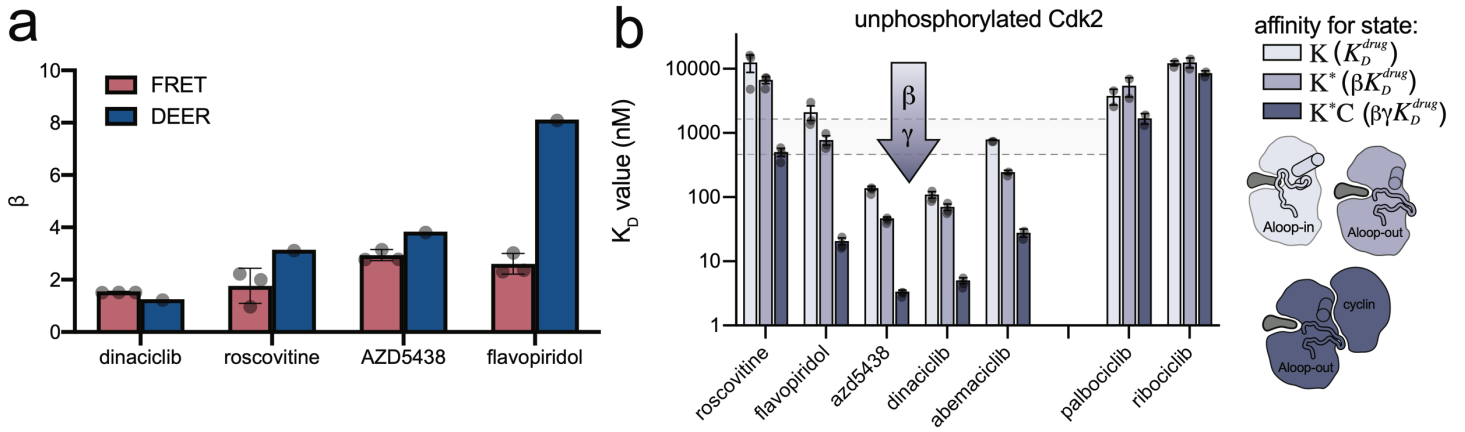
Supplementary Figure 6. DEER data on unphosphorylated Cdk2 bound to Cdk2 inhibitors (α C-helix). DEER spectra (bottom) and spin-spin distance distributions (top) for Cdk2 bound to four Cdk2 inhibitors. Distance distributions were acquired by fitting DEER spectra using Tikhonov regularization, and independently fitting to two Gaussian functions representing α C-out and α C-in states. The distance distribution from the α C-in state of Cdk2:K03861 is shown in grey and scaled along the y-axis for clarity. DEER spectra, Tikhonov fits and decomposed Gaussian fits are shown for a) Cdk2: dinaciclib, b) Cdk2: AZD5438, c) Cdk2: roscovitine, d) Cdk2: flavopiridol.



Supplementary Figure 7. The x-ray structure of monomeric Cdk2 bound to AZD5438 shows evidence of the inhibitor-driven conformational change. The two conformations in the crystallographic model (PDB ID: 6GUH) are colored light blue for the inactive state and dark blue for the active-like state. The position of the catalytic lysine K33 in the corresponding dinaciclib structure is shown in light yellow for comparison.

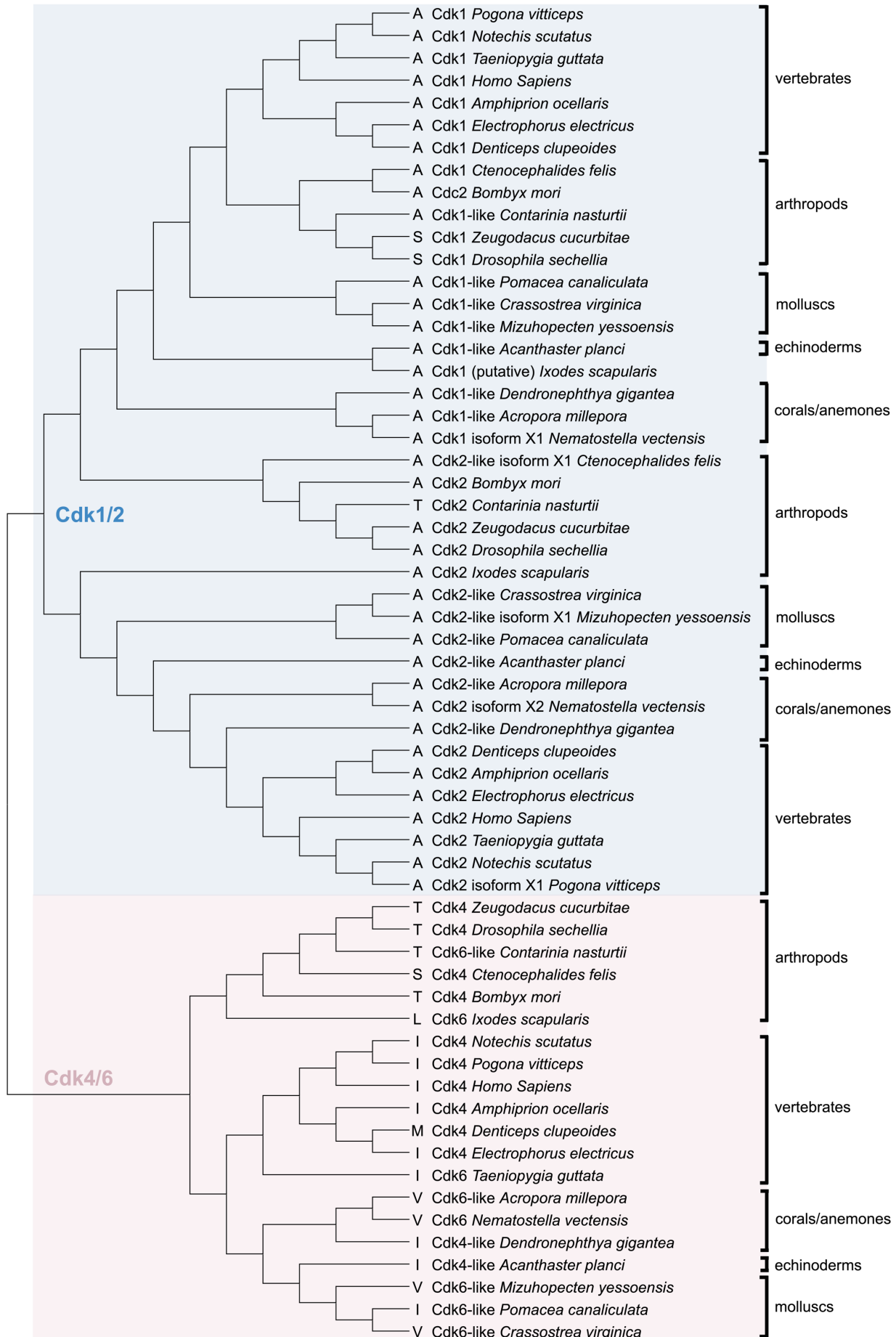


Supplementary Figure 8. FRET measurements of inhibitor binding. Inhibitor and cyclin binding experiments with **a**) unphosphorylated Cdk2 and **b**) phosphorylated Cdk2. Ratiometric FRET measurements from representative experiments are shown along with the global fits (dashed black lines, see Methods).

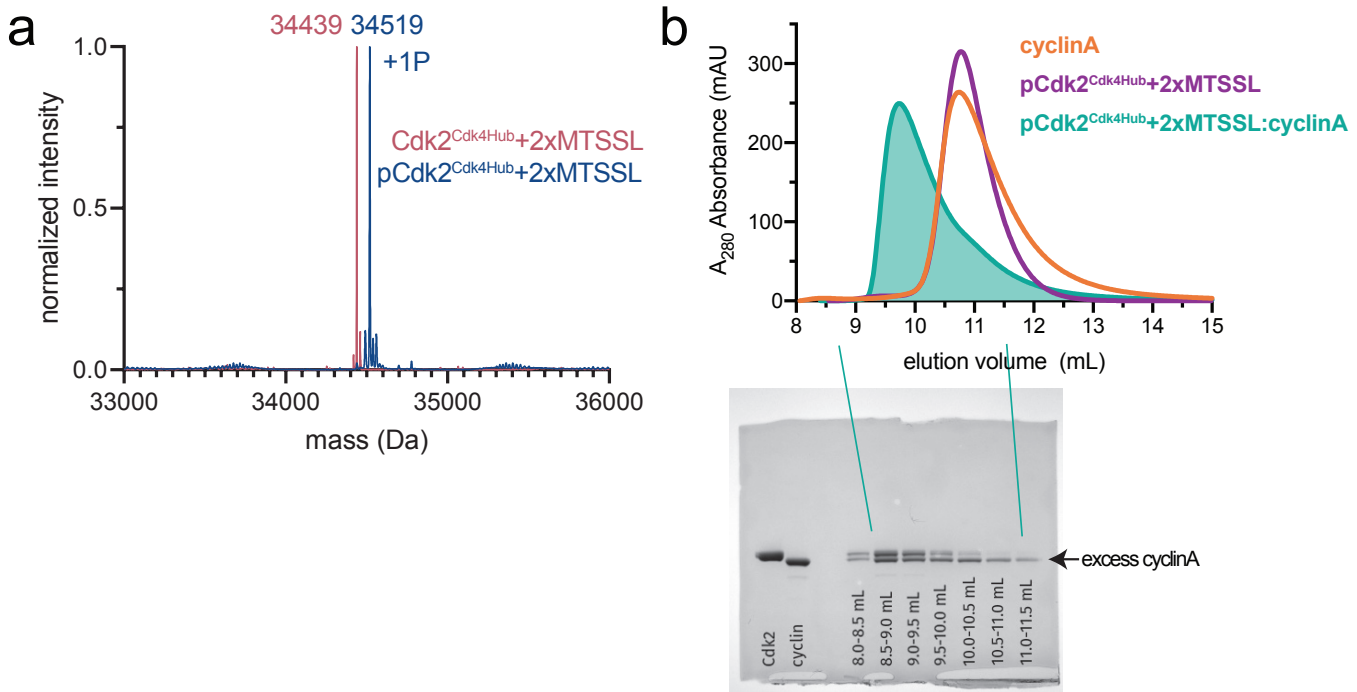


Supplementary Figure 9. Coupling parameters and microscopic equilibrium dissociation constants from the FRET analysis. a) β values derived from fits of the FRET data to the extended allosteric two state model (black) and the corresponding values independently measured with DEER (blue), show that the four Cdk2 inhibitors drive a conformational shift to the Aloop-out state. Values for FRET experiments are mean \pm S.E.M; n = 3 independent experiments **b)** Microscopic equilibrium dissociation constants for inhibitor binding to different conformational and biochemical states of unphosphorylated Cdk2. The corresponding data for phosphorylated Cdk2 are shown in main Figure 4d. Values are mean \pm S.E.M; n = 3 independent experiments

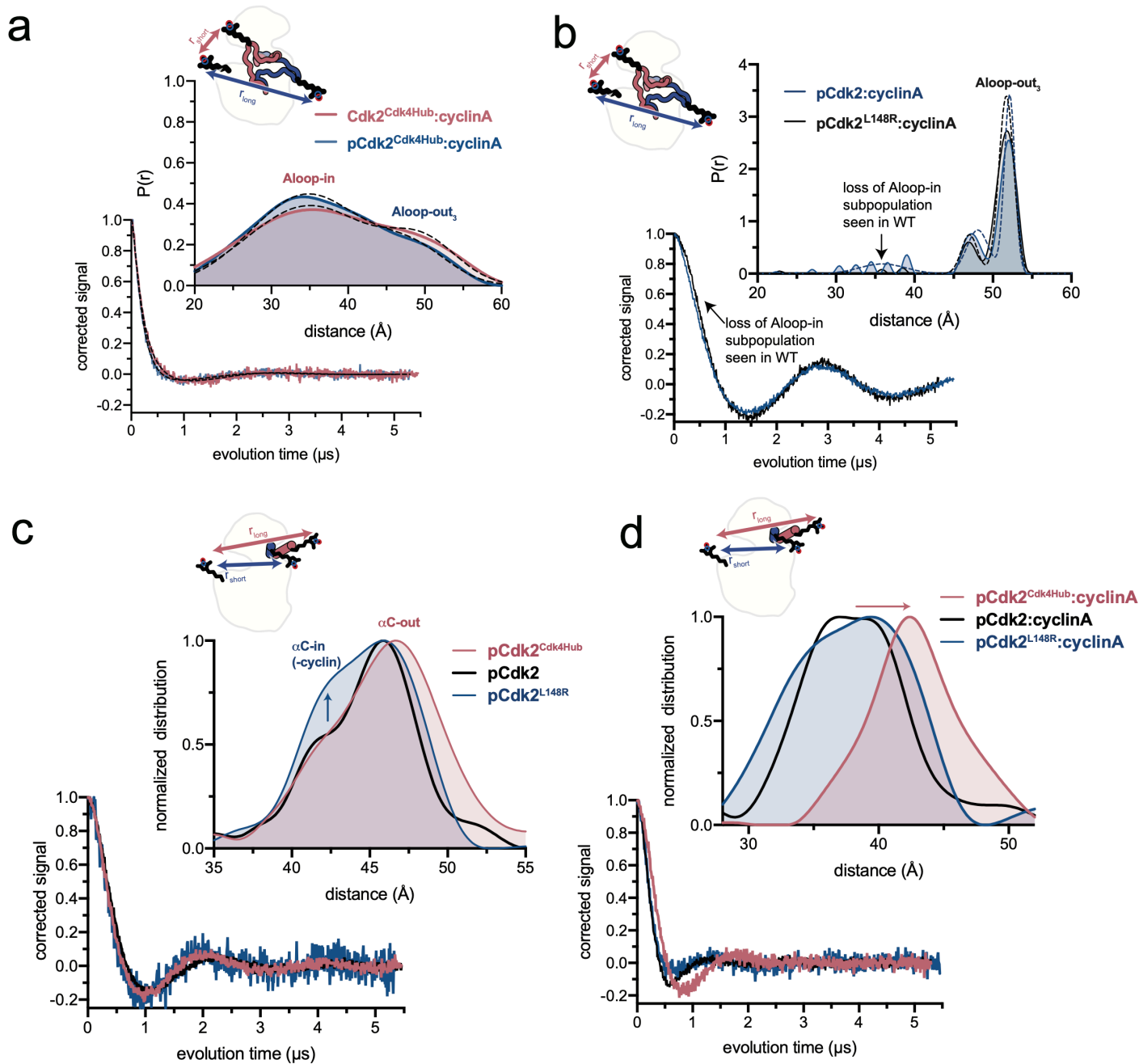
A151 in human Cdk2



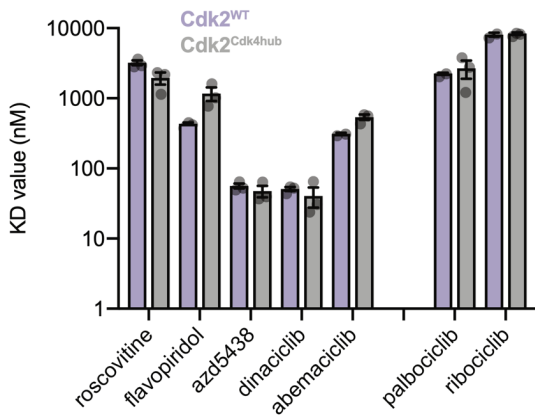
Supplementary Figure 10. Phylogenetic tree of Cdk1, Cdk2 and Cdk4/6 across metazoans. The phylogenetic tree was generated using the maximum likelihood method in MEGA X. The amino acid residue found at the central hub location (A151 in human Cdk2, I164 in human Cdk4) is shown for each species. There is a clear divergence of this position between Cdk2 and Cdk4 lineages.



Supplementary Figure 11. Validation of the Cdk2^{Cdk4Hub} construct, phosphorylation, cyclinA binding and folding. **a).** Mass spectrum of unphosphorylated and phosphorylated Cdk2^{Cdk4Hub} homogeneously labeled with 2 MTSSL spin labels (expected masses: 34439 Da and 34519 Da, respectively). **b)** Size exclusion chromatograms for spin-labeled monomeric Cdk2^{Cdk4Hub} (blue), MTSSL-labeled Cdk2^{Cdk4Hub}:cyclinA complex (green), and free cyclinA. The SDS-PAGE gel shows the fractions from the size exclusion run on the Cdk2^{Cdk4Hub}:cyclinA complex, confirming the formation of the 1:1 complex and demonstrating the presence of excess cyclinA in the sample used for DEER experiments. Protein samples used for reference Cdk2 and cyclinA markers (lanes 1 and 2) had been previously validated. This analysis was performed on the sample used for the DEER experiment.



Supplementary Figure 12. DEER spectra and distance distributions of the $Cdk2^{Cdk4Hub}$ and $Cdk2^{L148R}$ mutants. DEER spectra (below) and distance distributions (above) for **a**) unphosphorylated (red) and phosphorylated (blue) $Cdk2^{Cdk4Hub}$:cyclinA complexes. Unlike WT $Cdk2$, phosphorylation does not enhance the conformational shift to the Aloop-out₃ state in the mutant. **b**) $pCdk2$:cyclinA (blue) and $pCdk2^{L148R}$:cyclinA (black). The residual Aloop-in subpopulation observed in WT is lost in the L148R mutant, as manifested in the DEER spectra at early evolution times. **c**) monomeric $pCdk2$, $pCdk2^{Cdk4Hub}$ and $pCdk2^{L148R}$ showing that the L148R mutation drives a shift to the αC -in state. **d**) dimeric $pCdk2$:cyclinA, $pCdk2^{Cdk4Hub}$:cyclinA and $pCdk2^{L148R}$:cyclinA complexes, showing that cyclin and phosphorylation cannot drive $Cdk2^{Cdk4Hub}$ into the canonical αC -in conformation.



Supplementary Figure 13. Inhibitors do not discriminate well between the monomeric forms of WT Cdk2 and the $Cdk2^{Cdk4Hub}$ mutant. FRET binding affinities of Cdk2 and Cdk4 inhibitors for phosphorylated monomeric pCdk2 (blue) and pCdk2^{Cdk4Hub} (grey). Corresponding data for the phosphorylated pCdk2:cyclinA dimers are shown in main Figure 5h. The pronounced effects of the hub mutations on the affinities of the Cdk2 inhibitors for the dimer are not observed with the monomer, indicating that they arise from loss of allosteric coupling to the cyclin subunit in the $Cdk2^{Cdk4Hub}$ mutant. Values are mean \pm S.E.M; n = 3 independent experiments.

Supplementary Figure 14. Error surface analysis of global fitting of FRET data to the extended allosteric two state model. **a)** Gaussian populations derived from the DEER data for Cdk2 and Cdk2:cyclinA were used to constrain the values of the equilibrium constants K_{eq} and αK_{eq} in the fitting procedure. **b)** A representative error surface analysis of the fit parameters performed in Kintek Explorer. Every pairwise combination of unconstrained parameters was explored and the ratio of the optimal fit chi2 (chi2min) to the chi2 obtained with a given combination of parameters is plotted on a color scale as shown in the legend.